

# ADVANCED MATERIALS

## Supporting Information

for *Adv. Mater.*, DOI: 10.1002/adma.201504155

An Epidermal Stimulation and Sensing Platform for  
Sensorimotor Prosthetic Control, Management of Lower Back  
Exertion, and Electrical Muscle Activation

*Baoxing Xu, Aadeel Akhtar, Yuhao Liu, Hang Chen, Woon-  
Hong Yeo, Sung Il Park, Brandon Boyce, Hyunjin Kim, Jiwoo  
Yu, Hsin-Yen Lai, Sungyoung Jung, Yuhao Zhou, Jeonghyun  
Kim, Seongkyu Cho, Yonggang Huang, Timothy Bretl, and  
John A. Rogers\**

## Supporting Information

DOI: 10.1002/(adma.201504155)

Article type: Communication

### **An Epidermal Stimulation and Sensing Platform for Sensorimotor Prosthetic Control, Management of Lower Back Exertion, and Electrical Muscle Activation**

*Baoxing Xu<sup>†</sup>, Aadeel Akhtar<sup>†</sup>, Yuhao Liu<sup>†</sup>, Hang Chen, Woon-Hong Yeo, Sung II Park, Brandon Boyce, Hyunjin Kim, Jiwoo Yu, Hsin-Yen Lai, Sungyoung Jung, Yuhao Zhou, Jeonghyun Kim, Seongkyu Cho, Yonggang Huang, Timothy Bretl, John A. Rogers\**

Dr. Baoxing Xu

Department of Mechanical and Aerospace Engineering, University of Virginia, Charlottesville, VA 22904, USA. Departments of Materials Science and Engineering, Beckman Institute, and Frederick Seitz Materials Research Laboratory, University of Illinois at Urbana-Champaign, Urbana, IL 61801, USA.

Aadeel Akhtar

Neuroscience Program, Medical Scholars Program, Beckman Institute, and Coordinated Science Laboratory, University of Illinois at Urbana-Champaign, Urbana, IL 61801, USA.

Yuhao Liu, Dr. Sung II Park, Hyunjin Kim, Jiwoo Yu, Hsin-Yen Lai, Sungyoung Jung, Yuhao Zhou, Dr. Jeonghyun Kim, Seongkyu Cho, Prof. John A. Rogers  
Departments of Materials Science and Engineering, Beckman Institute, and Frederick Seitz Materials Research Laboratory, University of Illinois at Urbana-Champaign, Urbana, IL 61801, USA.

Prof. Woon-Hong Yeo

Department of Mechanical and Nuclear Engineering, Center for Rehabilitation Science and Engineering, Virginia Commonwealth University, Richmond, VA 23284, USA. Departments of Materials Science and Engineering, Beckman Institute, and Frederick Seitz Materials Research Laboratory, University of Illinois at Urbana-Champaign, Urbana, IL 61801, USA.

Hang Chen

Department of Engineering Mechanics and Center for Mechanics and Materials, Tsinghua University, Beijing 100084, China. Department of Mechanical Engineering and Department of Civil and Environmental Engineering, Center for Engineering and Health, and Skin Disease Research Center, Northwestern University, Evanston, IL 60208, USA

Brandon Boyce, Prof. Timothy Bretl

Departments of Aerospace Engineering, Beckman Institute, and Coordinated Science Laboratory, University of Illinois at Urbana-Champaign, Urbana, IL 61801, USA.

Prof. Yonggang Huang

Department of Mechanical Engineering and Department of Civil and Environmental Engineering, Center for Engineering and Health, and Skin Disease Research Center, Northwestern University, Evanston, IL 60208, USA.

†These authors contributed equally to this work

\*Corresponding-Author, Prof. John A. Rogers, e-mail: [jrogers@illinois.edu](mailto:jrogers@illinois.edu)

Keywords: Epidermal stimulation electronic system; Electrotactile stimulation; Surface electromyography (EMG); Electrical muscle stimulation

**Supplementary Note 1: Fabrication procedure for epidermal devices****Deposition of 1<sup>st</sup> layer Chrome/Gold**

1. Clean silicon wafer
2. Treat silicon wafer surface with Ultra-violet/ozone(UV-O) for 3mins
3. Spin coat PMMA (A2, 495)(2000rpm, 30s)
4. Anneal at 180°C for 3-4min
5. Spin coat PI(4000 rpm, 30s)
6. Anneal at 150°C for 5min
7. Anneal at 250°C under vacuum for 1 hr
8. Deposit 1<sup>st</sup> layer Cr(5nm)/Au(200nm) with electron beam evaporator

**1<sup>st</sup> mask (mask#1 Au) for temperature, strain and EMG sensors**

9. Spin coat PR AZ5214 (3000rpm, 30s)
10. Anneal at 110°C for 1-2min
11. Align mask#1 and expose with Karl Suss MJB3
12. Develop in developer AZ917
13. Anneal at 110°C for 3-4min
14. Etch Au with TFA Au etchant
15. Etch Cr with CR-7 Cr Mask Etchant
16. Remove PR with acetone/IPA/DI water

**2nd mask (mask#2 vias) for PI insulation layer:**

17. Spin coat PI(2000rpm, 30s)
18. Anneal at 150°C for 5min
19. Anneal at 250°C under vacuum for 1 hr
20. Spin coat PR AZ4620(2500rpm, 30s)
21. Anneal at 110°C for 3min
22. Align via mask#2 and expose with Karl Suss MJB3
23. Develop in developer AZ400K diluted with water 1:3
24. Etch exposed PI with March RIE.
25. Remove PR with acetone/IPA/DI water

**3rd mask (mask #3 Au) for electrodes**

26. Deposit Cr (8 nm)/Au (300 nm) with Sputter
27. Spin coat PR AZ5214 (3000rpm, 30sec)
28. Anneal at 110°C for 1-2min
29. Align mask#3 and expose with Karl Suss MJB3
30. Develop in developer AZ917
31. Anneal at 110°C for 3min
32. Etch Au with TFA Au etchant
33. Etch Cr with CR-7 Cr Mask Etchant
34. Etch exposed PI with March RIE
35. Remove PR with acetone/IPA/DI water

**4th mask (mask #4 PI) for the cover of strain and temperature sensors and connector wires and pads**

36. Spin coat PI(4000rpm, 30s)
37. Anneal at 150°C for 5min
38. Anneal at 250°C under vacuum for 1 hr

39. Spin coat PR AZ4620(2500rpm, 30s)
40. Anneal at 110°C for 3min
41. Align via mask#4 and expose with Karl Suss MJB3
42. Develop in developer AZ400K diluted with water 1:3
43. Etch exposed PI with March RIE
44. Remove PR with acetone/IPA/DI water

**Pickup using water-soluble tap**

45. Lift up device with acetone
46. Pick up device with water-soluble tape
47. Deposit Cr (5nm) and SiO<sub>2</sub> (60nm) with electron beam evaporator

**Transfer onto Ecoflex/PVA substrate**

48. Prepare Ecoflex/PVA substrate on glass wafer (coat PVA film onto glass wafer; spin coat Ecoflex (Part B:PartA, 2:1) (3000rpm, 120s); curl for one day at room temperature)
49. Prebake glass wafer with PVA and Ecoflex substrate
50. Treat Ecoflex/PVA substrate with Ultra-violet/ozone(UV-O) for 3min
51. Transfer device from water-soluble tape to Ecoflex/PVA substrate
52. Wash away water-soluble tape
53. Connect the ACF cable

**Supplementary Note 2: Circuit model and analysis of electrode on the skin**

The contact between electrode and skin can be described as a resistor and a capacitor in parallel. Supplementary Fig. S3a shows the equivalent circuit model, where  $R_{es}$  and  $C_{es}$  are the effective resistance and capacitance of the electrode-skin interface, respectively. When a constant current is supplied, a typical resistor–capacitor voltage step response curve is measured using both conventional electrodes and the epidermal device. Here, we take the charging phase for analysis<sup>1,2</sup>. Using the equation for capacitive charging, we can estimate the steady-state voltage, RC time constant, and the DC offset.

$$V(t) = (V_s - V_o) \times (1 - \exp^{-\frac{t}{\tau}}) + V_o$$

Where  $V_s$  is the steady-state voltage,  $V_o$  is the DC offset and  $\tau$  is the time constant for charging phase. The resistive part of the impedance can be computed by taking the steady-state voltage ( $V_s$ ), subtracting it from the DC offset ( $V_o$ ), and then dividing it by the stimulation current amplitude<sup>1,2</sup>. To account for the different sizes of electrodes, the resistance is normalized by multiplying the area of the electrode<sup>1</sup>:

$$R_{norm} = \frac{V_s - V_o}{I} \times area_{electrode}$$

The capacitive part can then be computed by dividing the resistance value from the estimate of  $\tau$ . To account for the different sizes of the electrodes, the capacitance is normalized by dividing by the area of the anode<sup>1</sup>:

$$C_{norm} = \frac{\tau}{R} \times \frac{1}{area_{electrode}}$$

The area of the conventional electrode was 263mm<sup>2</sup> and the area of the epidermal stimulation electrode was 3.14mm<sup>2</sup>.

**Supplementary Note 3a: Joule heat generation from current stimulation**

Supplementary Figure S4a shows the global IR camera images of the device onto the arm before and after 2-minute simulation with the current amplitude of 1.54 mA through one electrode. Even when the current stimulation is activated by two electrodes, the temperature rising is also localized in the contact areas between electrodes and skin, as shown in Supplementary Figure S4b. Finite element analysis (FEA) is used to study the temperature increase in the device due to the joule heating. The device, which is modeled by the heat transfer shell elements (DS4, ABAQUS<sup>3</sup>), with the substrate (Ecoflex, ~30um in thickness, thermal conductivity ~0.16 W/mK, modeled by the heat transfer brick elements (DC3D8, ABAQUS<sup>1</sup>)) is mounted, and therefore in direct contact with, the skin tissues. Their thickness and thermal properties are given in Supplementary Table S1. The temperature at the bottle of the muscle layer has a constant body temperature 37 °C due to heating of the blood. The upper surface of the substrate has natural convection with air, where the convective heat transfer coefficient is 13 W/m<sup>2</sup>K.<sup>4</sup> The room temperature is taken from Supplementary Figure S4a as 21 °C. The temperature of the substrate surface exposure to air is 30 °C with none electrodes activated, which is consistent with the experiment as show in Supplementary Figure S4b. The power for each electrode is calculated by  $P=\eta UI$ , where  $U$  and  $I$  are the stimulation current and the measured voltage respectively, and  $\eta$  is the ratio of current pulse time to its period. Supplementary Figure S4c shows the temperature distribution in the whole device at steady state; where only left half of the device is shown as two symmetrical electrodes are activated. The bottom left magnified view shows the temperature in the electrode; the average increase is ~0.002 °C. The bottom right magnified view shows temperature in the strain sensor; its temperature change is less than 0.0001 °C, which is consistent with the experiments that no temperature change is captured by global IR camera images, and confirms that the Joule heating due to stimulation will not affect the strain measurement.

**Supplementary Table S1. The thickness and thermal properties of various tissues under the device.**

Parameters	Skin	Fat	Muscle
Desity (kg/m <sup>3</sup> ) <sup>5-8</sup>	1085	850	1085
Specific heat capacity (J/kg K) <sup>5-8</sup>	3680	2300	3768
Thermal conductivity (J/m K) <sup>5-8</sup>	0.47	0.16	0.42
Thickness (mm) <sup>7-10</sup>	1.0	4.4	13.6

**Supplementary Note 3b: FEA analysis on mechanical deformation**

FEA is also carried out to study the effects of mechanical deformation of this stretchable device on both the temperature and EMG measurements. The silicone elastomer (Ecoflex,  $\sim 30\ \mu\text{m}$  in thickness, with modulus  $\sim 60\ \text{kPa}$ ) is modeled by the hexahedron element (C3D8R, ABAQUS<sup>1</sup>), while the device is modeled by the composite shell element (S4R, ABAQUS<sup>1</sup>). Supplementary Figure S5a shows the strain distribution in the Au layer of the device under 21% stretch, where the maximum strain occurs at the joint of the electrode to wires and is less than 0.3% (yield strain of gold), which indicates that the device can sustain larger, cyclic stretch without plastic deformation. The normal strain distributions in the horizontal (x) and vertical (y) directions in the temperature sensor are shown in Supplementary Figure S5b. For the average normal strain (-0.07%) in y direction, the average change in the electrical resistance of the temperature sensor is equivalent to that for  $-0.09\ ^\circ\text{C}$  temperature change, which is much smaller than that due to muscle reaction during subsequent experiments ( $\sim 2\ ^\circ\text{C}$ ). Due to the Poisson's effect (vertical contraction for horizontal stretch) of the substrate, the EMG buckles into sinusoidal deformation in the out-of-plane direction to minimize the strains, as show in Supplementary Figure S5c. The maximum strain in the EMG is as small as 0.09% due to its meshed serpentine structure, which indicates a negligible effect of mechanical deformation on EMG measurements.



## **Supplementary Note 4a: Robot teleoperation-gripping water bottle**

One of humanoid robot hands (Baxter, Rethink Robotics)) is to mimic a virtual hand. The object to be gripped is a plastic bottle with water and the water is helpful to monitor deformation of bottle. A very thin force sensor is attached inside of robot hand gripper to extract the gripping force of gripper applied to the bottle through a computer. Epidermal device was mounted on the forearm of the subject volunteer (male, 23years old), and the subject was asked to flex his forearm with elbow on the table.

## **Supplementary Note 4b: Fatigue test on arm muscle groups**

The epidermal device was mounted on the skin of arm of a subject volunteer (male, 23years old). He was asked to hold a 20lb weight in hand as long as he could. The EMG and temperature measurements were carried out to simultaneously record the data for analysis. The EMG amplitude shows an obvious decrease while the temperature shows an obvious increase as a function of measurement time.

**Supplementary Note 5: Robot teleoperation-Rotation of elbow**

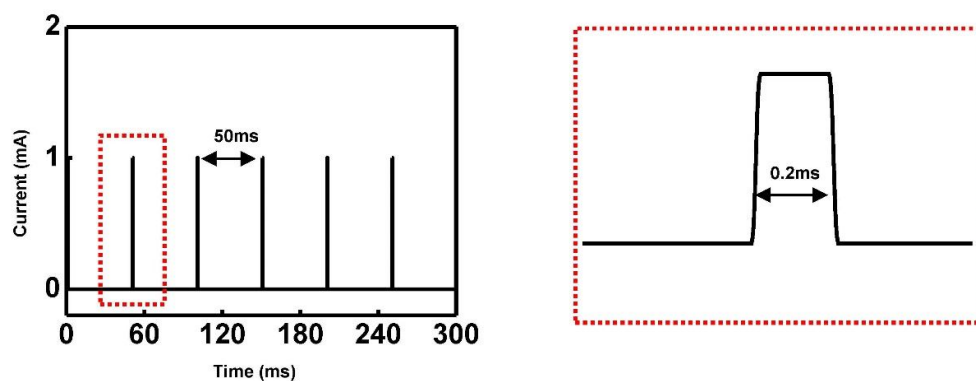
Two epidermal devices were attached on the upper arm of the subject volunteer (male, 23years old). One was on biceps and the other was on triceps. Two electrodes on the biceps epidermal device were chosen to send current stimulation. The subject was asked to place his forearm in parallel with the table and the hand was held tightly on a supporter. When he try to lift the support up, the biceps was activated, generating EMG signals. When he compressed the support down, the triceps was activated, generating EMG signals as well. He was asked to lift up and compress down the support back and forth, EMG signals were generated alternatively, driving the virtual elbow rotation. The subject was trained before test, referred to as offline training process, and was asked to get the knowledge of one-to-one correspondence between stimulation sensation (position and intensity) and elbow position. In the practical test, referred to as online process, the subject would try to match positions of the virtual arm based on his training experience (guess) and the given-target. The conventional electrodes and stimulation pads were mounted on the biceps and triceps to perform the test separately for comparison.

**Supplementary Note 6: Fatigue test on low back muscle**

A volunteer (male, 23years old) was first asked to lay on his stomach on a table with the epidermal device mounted on the skin of low back. He was then asked to hold a 20lb weight in the hands, and the volunteer was first flex his back with angle of 26° to the table (i.e. ground). The EMG and temperature measurements were performed to simultaneously record the data for analysis. The EMG barely shows any change, but the temperature behaves an obvious increase.

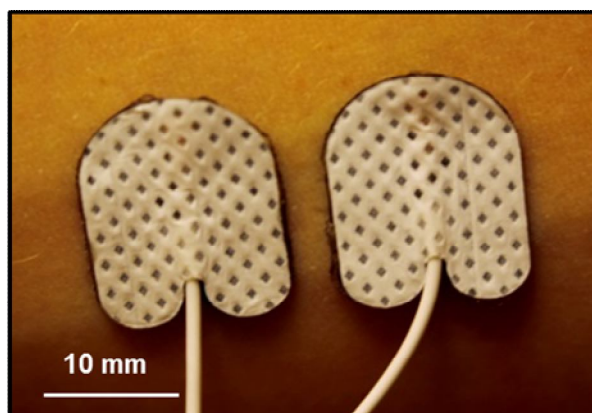
**References:**

- 1 K. A. Kaczmarek, J. G. Webster, P. Bach-y-Rita, W. J. Tompkins, *IEEE Trans. Biomed. Eng.* **1991**, 38, 1.
- 2 T. Keller, A. Kuhn, *J. Automat. Contr.* **2008**, 18, 35
- 3 ABAQUS. Analysis user's manual v.6.9. Pawtucket, RI: Dassault Systèmes, **2009**.
- 4 Incropera, F. P., DeWitt, D.P., Bergman, T.L., Layine, A.S. Fundamentals of Heat and Mass Transer, Wiley, Hoboken. **2007**.
- 5 C. Deshpande, Thermal analysis of vascular reactivity. MS thesis, Texas A&M University, **2007**.
- 6 D. Fiala, K.J. Lomas, M. Stohrer, *J. Appl. Physiol.* **1999**, 87, 1957.
- 7 R. C. Webb, A. P. Bonifas, A. Behnaz, Y. Zhang, K. J. Yu, H. Cheng, M. Shi, Z. Bian, Z. Liu, Y.-S. Kim, W.-H. Yeo, J. S. Park, J. Song, Y. Li, Y. Huang, A. M. Gorbach, J. A. Rogers, *Nat. Mater.* **2013**, 12, 938.
- 8 W.J. Song, S. Weinbaum, L.M. Jiji, D. Lemons, *J.Biomech. Eng.* **1988**, 110, 259.
- 9 P. Sieg, S.G. Hakim, S. Bierwolf, D.Hermes, *Int. J.Oral Maxillo. Surg.* **2003**, 32, 544.
- 10 H. Shen, J.R. Long, D.H. Xiong, Y.F. Guo, P. Xiao, Y.Z. Liu, L.J. Zhao, Y.J. Liu, H.Y. Deng, J.L. Li, R.R. Recker, H.W. Deng, *J. Med. Genet.* **2006**, 43, 873.

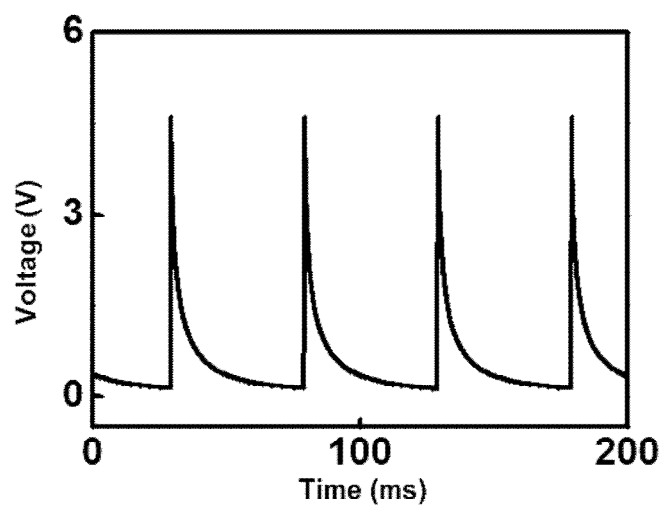


**Supplementary Figure S1:** 20Hz constant current positive monophasic square pulses used for electrotactile stimulation. A series of pulses is shown on the left with a magnified single pulse shown on the right.

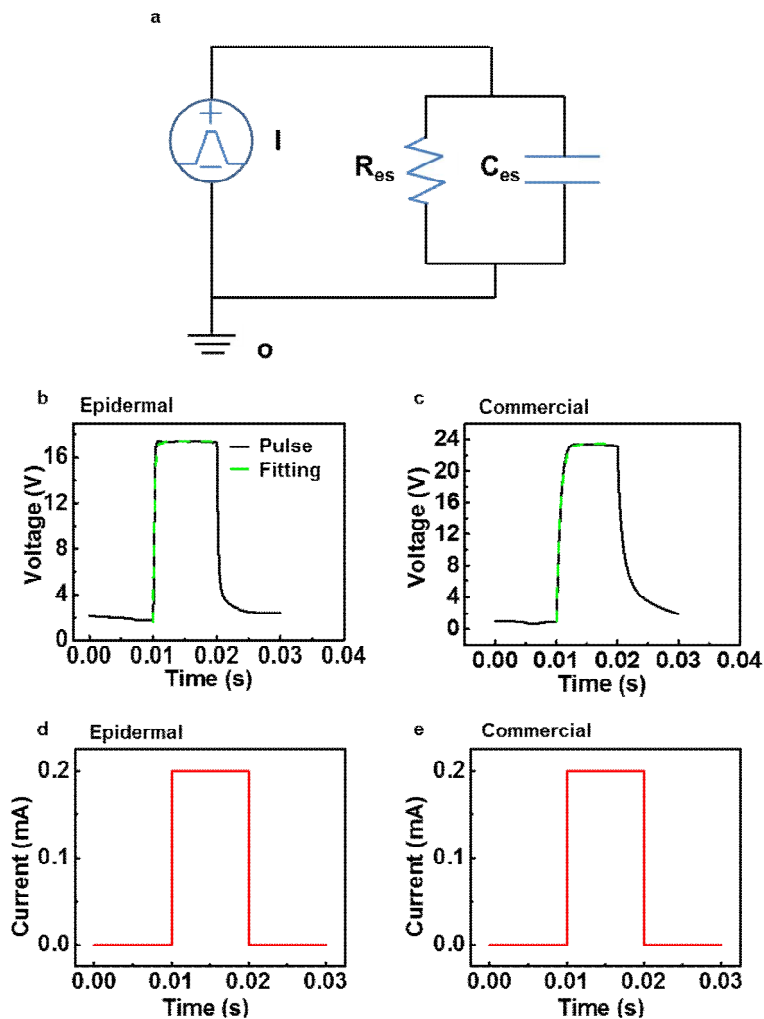
a



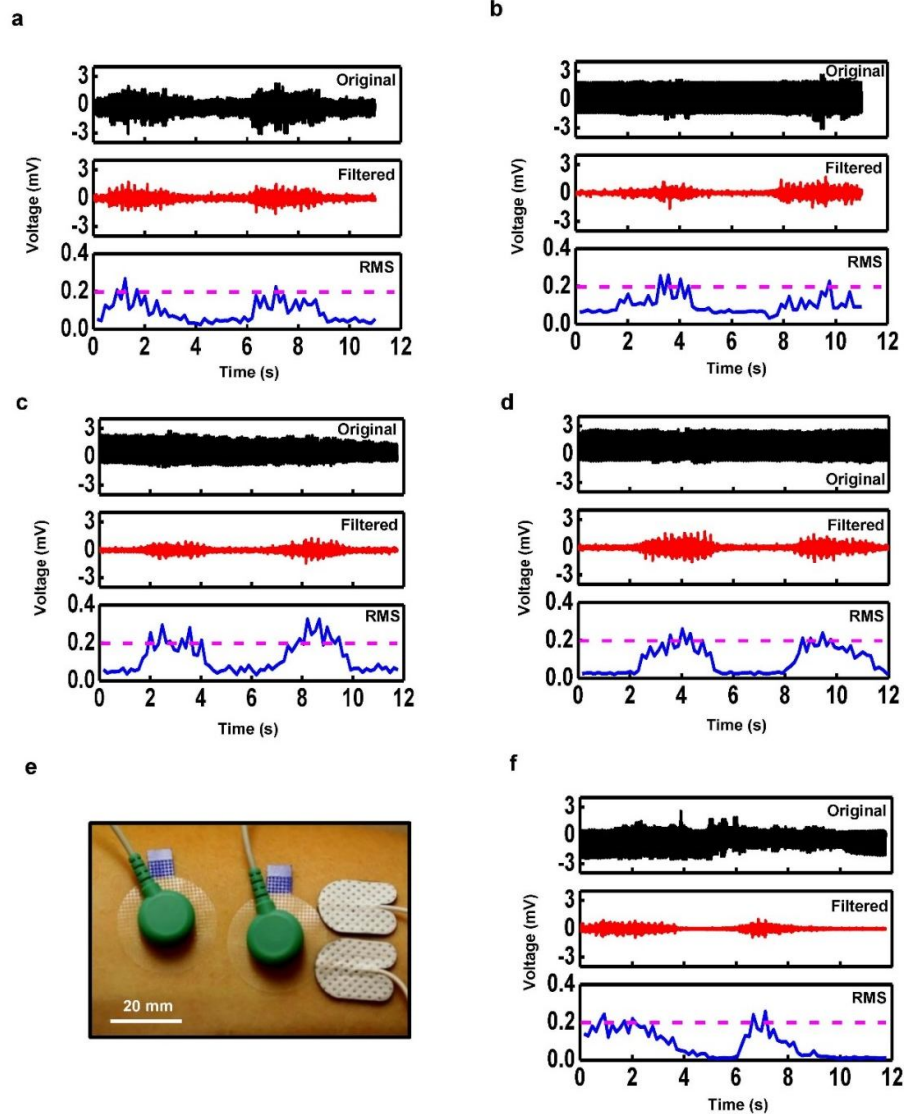
b



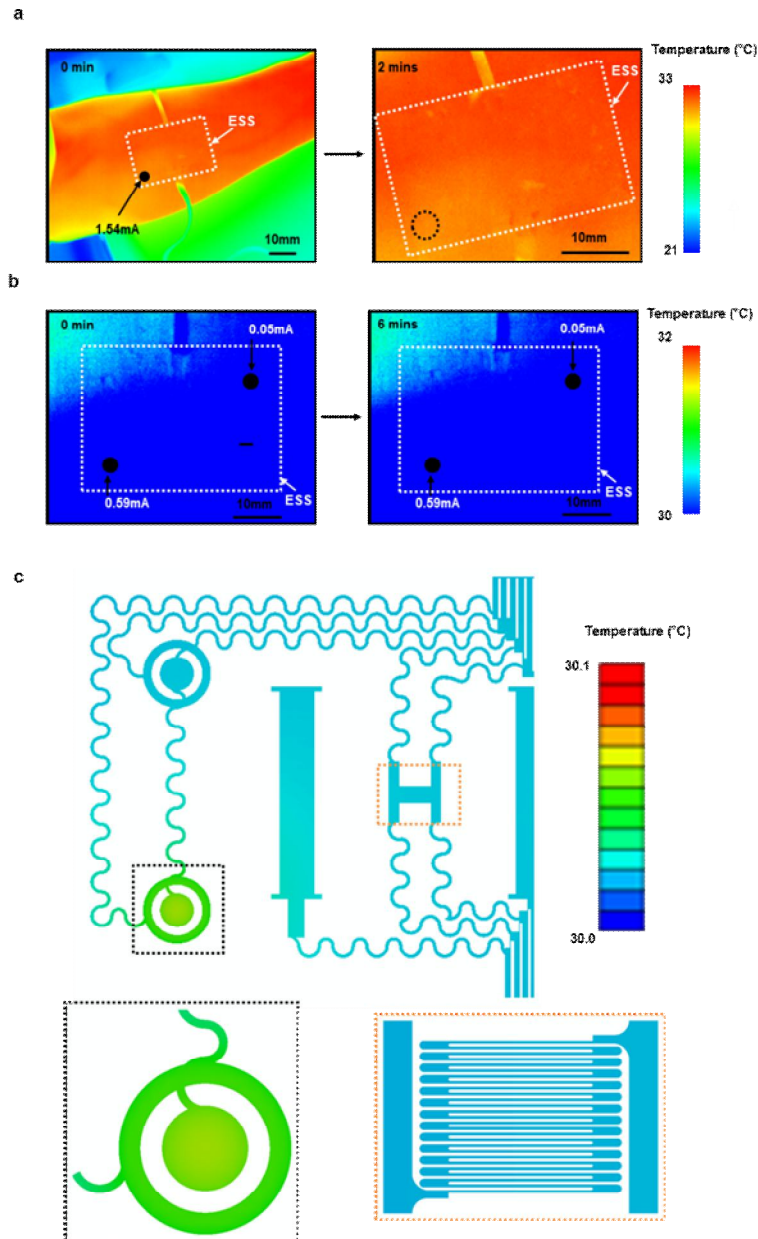
**Supplementary Figure S2: Conventional electrodes used in stimulation.** (a) Image of the conventional electrodes placed on the skin. (b) Representative measured voltage during 20Hz stimulation at 3mA.



**Supplementary Figure S3:** (a) Simplified electrical model for the electrode-skin impedance with  $R_{ec}$  and  $C_{ec}$ . (b) Voltage pulse applied to the concentric epidermal current stimulation electrode with area of  $3.14\text{mm}^2$  and (c) commercial hydrogel electrode with area of  $263\text{ mm}^2$ . Current stimulation profile of (d) epidermal electrode and (d) commercial hydrogel electrode.

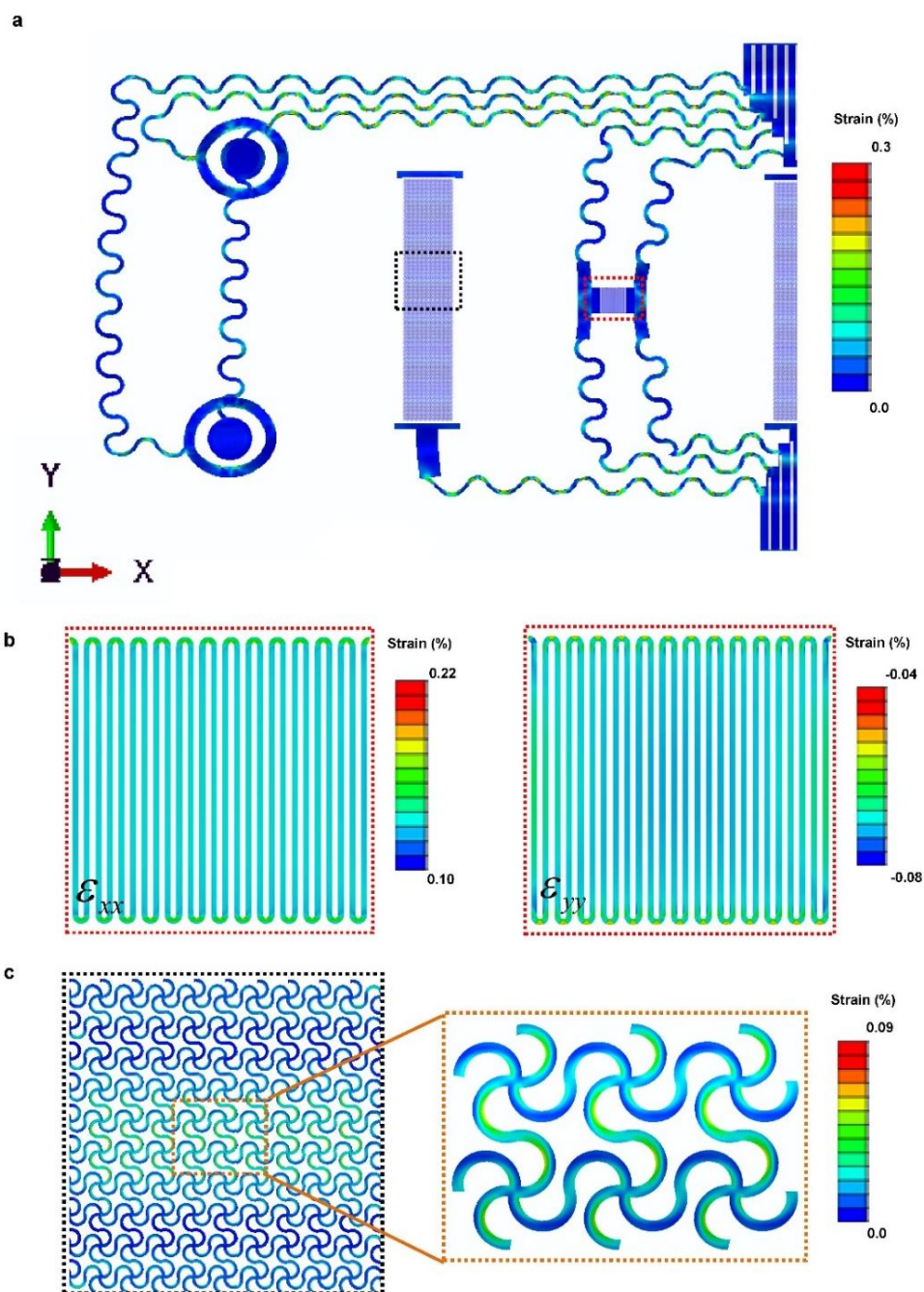


**Supplementary Figure S4: Effects of stimulation on EMG measurements taken simultaneously through the epidermal device and conventional electrodes.** (a) EMG recorded on the epidermal device during 20Hz constant current stimulation at electrode 1, (b) 20Hz stimulation at electrode 2, (c) 50Hz stimulation at electrode 1, and (d) 10Hz stimulation at electrode 1. The top plots shows the original EMG signal, the middle shows the filtered signal removing stimulation artifacts, and the bottom shows the root mean square (RMS) of the filtered EMG signal. (e) Image of simultaneous electrotactile stimulation and EMG recording using conventional stimulation electrodes (white) and conventional EMG sensors (green). (f) EMG recorded from conventional EMG sensors during 20Hz stimulation using conventional stimulation electrodes.



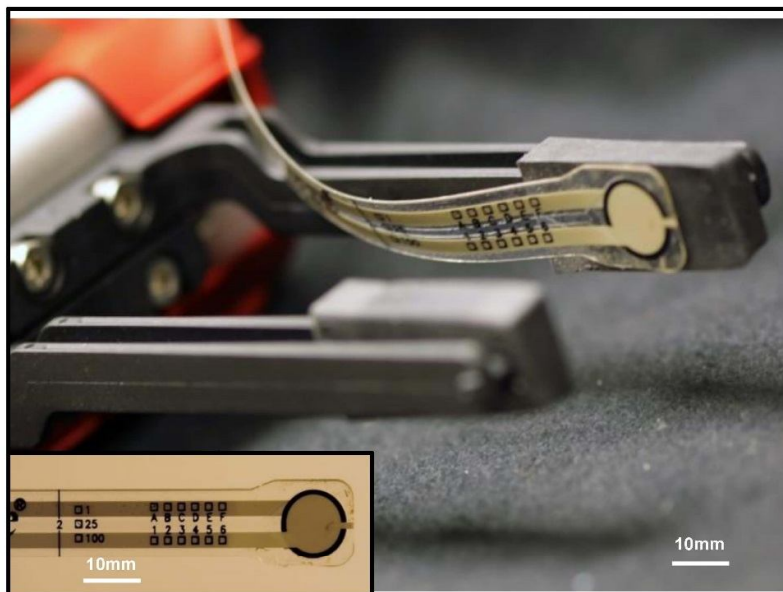
**Supplementary Figure S5: Experimental studies and finite element analysis (FEA) of the temperature sensor on the epidermal device when stimulation is active. (a)** Infrared images during stimulation from an electro-tactile stimulation electrode on the epidermal device placed on the forearm. The left image shows the temperature distribution before stimulation, and the right shows the temperature distribution after 20Hz stimulation at 1.54mA for 2 minutes. **(b)** Infrared images during stimulation from two electro-tactile stimulation electrodes on the epidermal device placed on the forearm. The left image shows the temperature distribution before stimulation, and the right shows the temperature distribution after 20Hz stimulation at 0.59mA for electrode 3 and 0.05 mA for electrode 2 for 6 minutes. **(c)** FEA results of temperature at steady state during stimulation from two symmetric electrodes with current of 1.54mA. The magnified view (bottom left) shows the temperature distribution at steady state on the electrode with an average increase  $\sim 0.5^{\circ}\text{C}$ . The magnified view (bottom right) shows the temperature distribution at steady state on the strain sensor. There is no temperature change, indicating that the Joule heating due to stimulation will not affect the strain measurement.



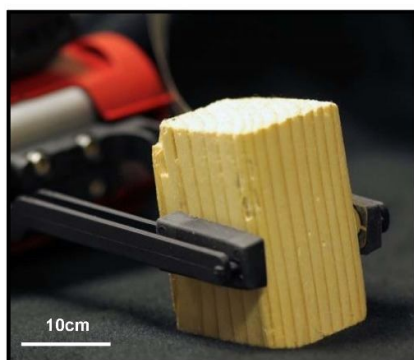


**Supplementary Figure S6: Mechanical Finite Element Analysis of the epidermal device.** (a) Strain distribution of the epidermal device at 21% stretch. Maximum strain occurs at the junction of the electrode and connector wires. (b) Magnified view of the strain distribution on the temperature sensor in x and y directions. (c) Magnified view of the strain distribution on the EMG sensor.

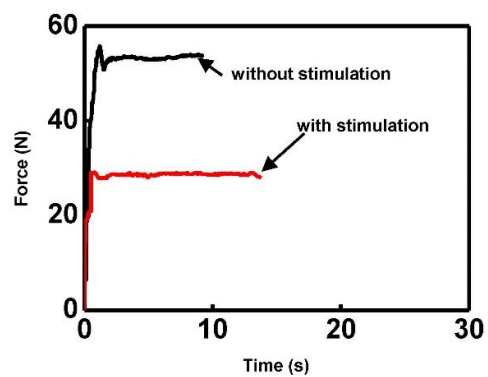
a



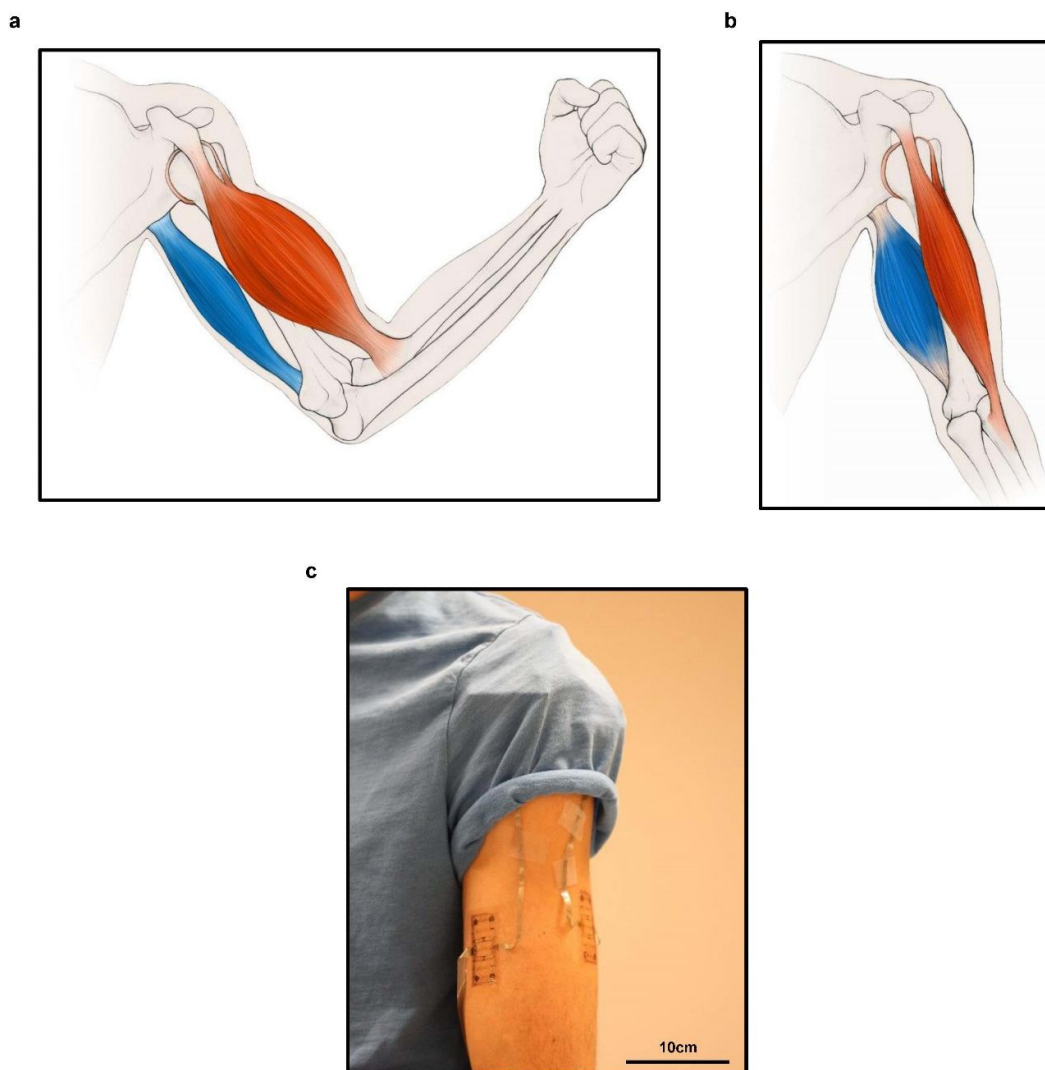
b



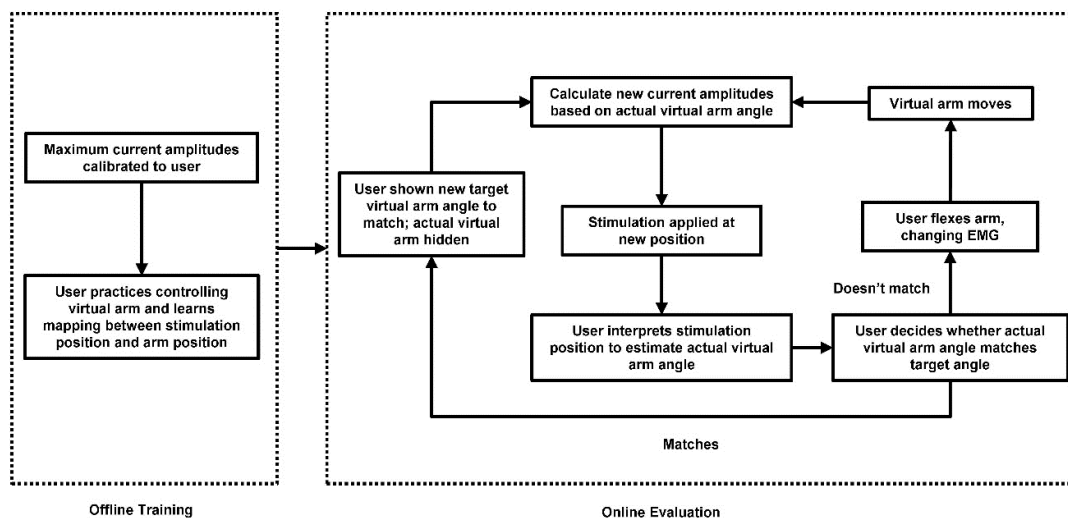
c



**Supplementary Figure S7: Control of robot gripping a block of wood while receiving electro-tactile force feedback.** (a) Image of robot gripper with force sensor (inset, magnified view). (b) Image of the block of wood being gripped. (c) Corresponding recorded gripping force.

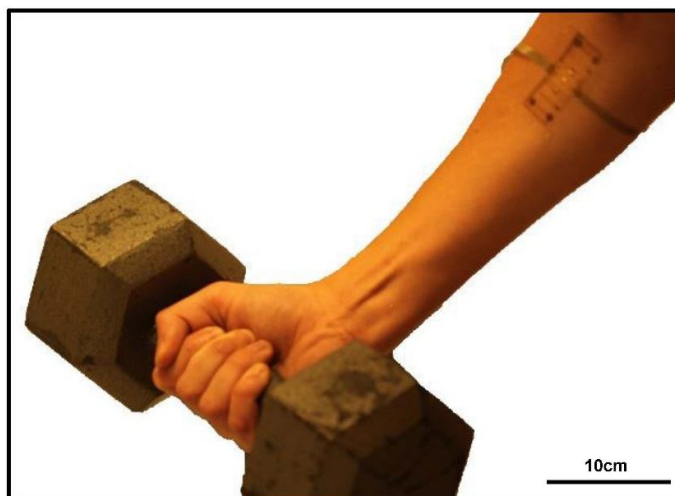


**Supplementary Figure S8: Schematics of muscle activity to elicit EMG recorded by the epidermal devices on the biceps and triceps brachii muscles.** (a) During elbow flexion, the biceps contract and triceps relax d. (b) During elbow extension, the triceps contract and the biceps relax. (c) Image of the epidermal devices on the biceps and triceps.

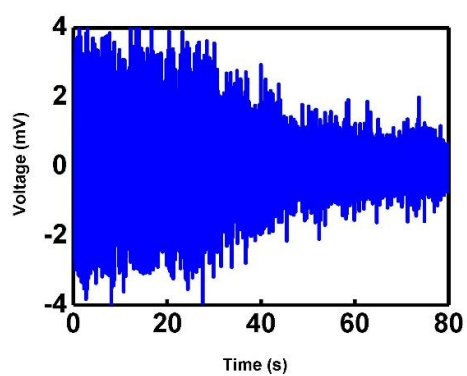


**Supplementary Figure S9:** Diagram detailing the experimental protocol used in the virtual arm targeting task.

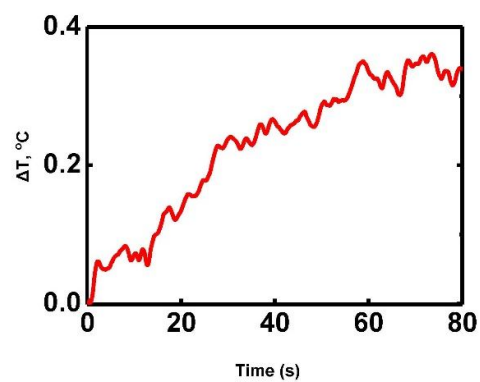
a



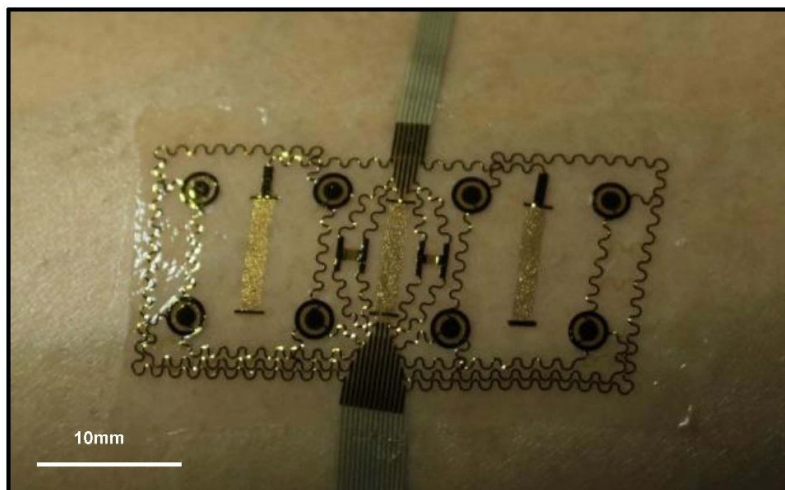
b



c



**Supplementary Figure S10: Measurements of muscle fatigue on the forearm.** (a) Image of the epidermal device on the forearm of the subject holding a 20lb weight for 80s. (b) Corresponding recorded EMG. (c) Corresponding recorded temperature.

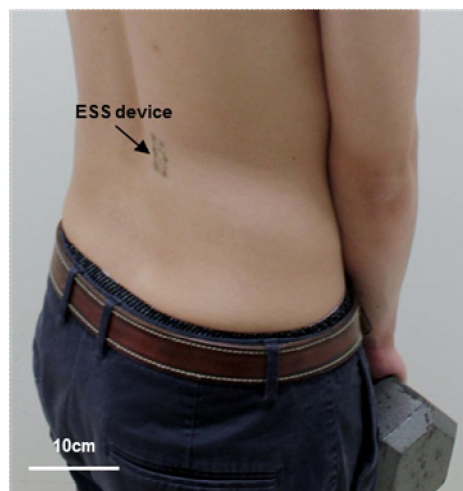


**Supplementary Figure S11:** Image of an epidermal device mounted on the skin with a higher stimulation electrode density.

a

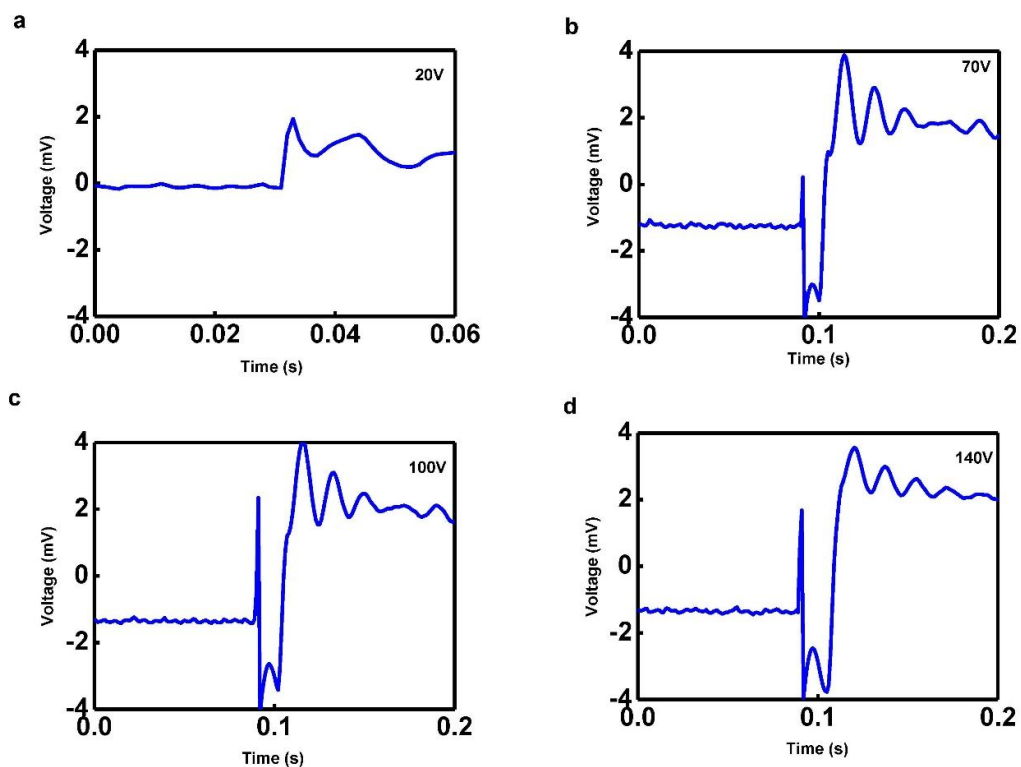


b



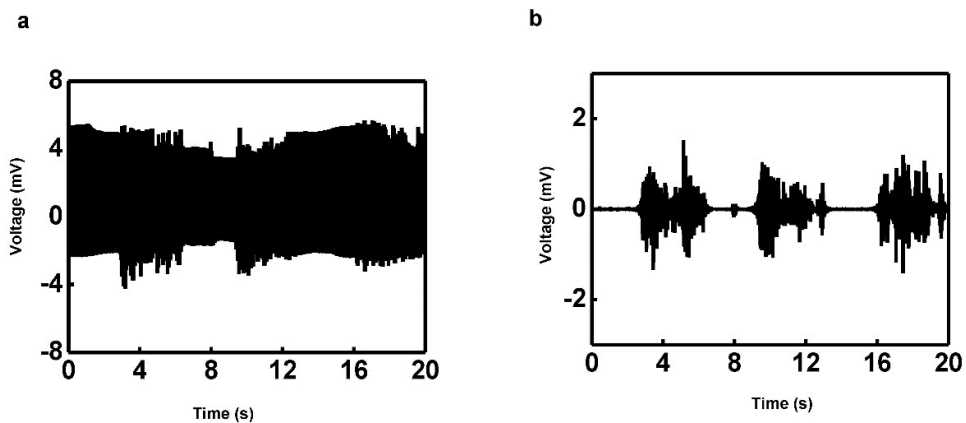
**Supplementary Figure S12: Schematic of lower back pain detected using the epidermal device.** (a) Overstretching of lower back muscles when stooping to lift an object. (b) Image of epidermal device mounted on the lower back.





**Supplementary Figure S13: Representative M-wave during a single pulse at different stimulation voltage amplitudes through an enhanced epidermal device on the skin. (a) 20V. (b) 70V. (c) 100V. (d) 140V.**





**Supplementary Figure S14: Recorded EMG signals during electrical muscle stimulation through an enhanced epidermal device. (a) Raw EMG signal containing stimulation artifact and M-waves during 20Hz muscle stimulation at 50V. (b) Recovered voluntary EMG signals after filtering out stimulation artifacts and M-waves.**